Measurement of the $e^+e^- \to K_S K_L \pi^0$ cross section in the energy range $\sqrt{s} = 1.3$–2.0 GeV

M. N. Achasov,[1,2] V. M. Aulchenko,[1,2] A. Yu. Barnyakov,[1,2] K. I. Beloborodov,[1,2] A. V. Berdyugin,[1,2] D. E. Berkaev,[1,2] A. G. Bogdanchikov,[1] A. A. Botov,[1] T. V. Dimova,[1,2] V. P. Druzhinin,[1,2] V. B. Golubev,[1,2] L. V. Kardapoltsev,[1,2] A. S. Kasaev,[1] A. G. Kharlamov,[1,2] A. N. Kirpotin,[1] I. A. Koop,[1,2,3] L. A. Korneev,[1,*] A. A. Korol,[1,2] D. P. Kovrizhin,[1] S. V. Koshuba,[1] A. S. Kupich,[1,2] N. A. Melnikova,[1,2] K. A. Martin,[1] A. E. Obrazovsky,[1] A. V. Otboev,[1] E. V. Pakhtusova,[1] K. V. Pugachev,[1,2] Yu. A. Rogovsky,[1,2] A. I. Senchenko,[1,2] S. I. Serednyakov,[1,2] Z. K. Silagadze,[1,2] Yu. M. Shatunov,[1,2] D. A. Shtol,[1] D. B. Shwartz,[1,2] I. K. Surin,[1] Yu. V. Usov,[1] and A. V. Vasiljev[1,2]

[1]*Budker Institute of Nuclear Physics, SB RAS, Novosibirsk, 630090, Russia*
[2]*Novosibirsk State University, Novosibirsk 630090, Russia*
[3]*Novosibirsk State Technical University, Novosibirsk 630092, Russia*

(Received 21 November 2017; published 20 February 2018)

The $e^+e^- \to K_S K_L \pi^0$ cross section is measured in the center-of-mass energy range $\sqrt{s} = 1.3$–2.0 GeV. The analysis is based on the data sample with an integrated luminosity of 33.5 pb^{-1} collected with the SND detector at the VEPP-2000 e^+e^- collider.

DOI: 10.1103/PhysRevD.97.032011

I. INTRODUCTION

This paper is dedicated to the study of the reaction $e^+e^- \to K_S K_L \pi^0$. This reaction is one of three charge modes of the process $e^+e^- \to K\bar{K}\pi$, which gives a sizable contribution to the total cross section of e^+e^- annihilation into hadrons in the center-of-mass energy range $\sqrt{s} = 1.5$–1.8 GeV. The process $e^+e^- \to K\bar{K}\pi$ is also important for the spectroscopy of $s\bar{s}$ vector states. From these states, only the lowest $\phi(1020)$ is well studied. In particular, its branching fractions are measured up to 10^{-5} level. Spectroscopy of the first excited state $\phi(1680)$ is far from completion. The main decay mode of $\phi' \equiv \phi(1680)$ is $K^*(892)\bar{K}$[1] with the $K^*(892)$ decay to $K\pi$.

Processes of e^+e^- annihilation to the $K\bar{K}\pi$ final state were studied in the DM1, DM2, and *BABAR* [1–4] experiments. Until recently, only the two subprocesses $e^+e^- \to K_S K^\pm \pi^\mp$ and $K^+K^-\pi^0$ [3] were measured. The third, neutral subprocess $e^+e^- \to K_S K_L \pi^0$ is hard to study due to the complexity of K_L-meson detection and identification. Recently, it was measured in the *BABAR* experiment [4]. The measurement uses the initial state radiation method, in which the $e^+e^- \to X$ cross section is determined from the mass spectrum of the hadron system X in the reaction $e^+e^- \to X\gamma$. Detection of all final particles in the reaction $e^+e^- \to K_S K_L \pi^0 \gamma$ was required, and the K_L meson was identified as a single photon. The efficiency of K_L-meson detection was measured using $e^+e^- \to \phi(1020)\gamma \to K_S K_L \gamma$ events selected without any conditions on K_L parameters. It should be noted that the K_L-meson energy was not measured. Therefore, good background suppression was not reached in Ref. [4]. A relatively large systematic uncertainty of the $e^+e^- \to K_S K_L \pi^0$ cross-section measurement ($\sim$10% at the cross-section maximum) is due to an uncertainty in background subtraction.

In this paper, the process $e^+e^- \to K_S K_L \pi^0$ is studied using a data sample collected in the energy range $\sqrt{s} = 1.3$–2.0 GeV with the SND detector [5] at the VEPP-2000 e^+e^- collider [6].

II. DETECTOR AND EXPERIMENT

SND is a general purpose nonmagnetic detector. Its main part is a three-layer electromagnetic calorimeter based on NaI(Tl) crystals. The calorimeter covers a solid angle of 95% of 4π. Its energy resolution is $\sigma_{E_\gamma}/E_\gamma = 4.2\%/\sqrt[4]{E_\gamma(\mathrm{GeV})}$, while the angular resolution is $\sigma_{\theta,\phi} = 0.82°/\sqrt{E_\gamma(\mathrm{GeV})}$, where E_γ is the photon energy. The tracking system is located inside the calorimeter, around the collider beam pipe. It consists of a nine-layer cylindrical drift chamber and a proportional chamber with cathode-strip readout. A solid angle covered by the tracking system is 94% of 4π. For charged kaon identification, a system of threshold aerogel Cherenkov counters is used.

*leonidkorneev@gmail.com

[1]Throughout this paper, the use of charge conjugate modes is implied.

The calorimeter is surrounded by a muon system consisting of proportional tubes and scintillation counters.

The analysis uses a data sample with an integrated luminosity of 33.5 pb^{-1} recorded in 2010–2012 in the energy region 1.3–2.0 GeV. Due to relatively small statistics of selected events of the process under study, data collected in the 36 energy points are combined into 15 energy intervals, as listed in Table I.

The simulation of the process $e^+e^- \to K_S K_L \pi^0$ is performed using a Monte Carlo (MC) event generator based on formulas from Ref. [7]. It is assumed that the process proceeds via the $K^*(892)^0\overline{K}^0$ intermediate state.

Interaction of particles produced in e^+e^- collision with the detector material is simulated using the GEANT4 v.9.5 package [8]. Analyses of processes with a K_L meson in the final state critically depend on correct simulation of K_L nuclear interaction. Unfortunately, both the total and inelastic low-energy cross section of the K_L nuclear interaction are strongly overestimated in GEANT4 v.9.5 [9]. Therefore, we have modified the GEANT4 module responsible for K_L cross-section calculation using the model from Ref. [10]. This model describes reasonably well the experimental data both on the total K_L cross section in different materials (H, Be, C, Al, Fe, Cu, Pb) in the K_L energy range 525–600 MeV [11] and on the inelastic cross section in the range 510–700 MeV [9]. Accuracy of the model is estimated by comparison of its prediction with the precisely measured value of the K_L inelastic cross section at 510 MeV [9] and is found to be about 12%.

The simulation takes into account the variation of experimental conditions during data taking, in particular dead detector channels, the size and position of the collider interaction region, beam-induced background, etc. The beam background leads to the appearance of spurious photons and/or charged particles in data events. To take this effect into account in simulation, special background events are recorded during data taking with a random trigger. These events are then superimposed on simulated events.

In this paper the reaction $e^+e^- \to K_S K_L \pi^0$ is studied in the decay mode $K_S \to 2\pi^0$, with no charged particles in the final state. Therefore, the process $e^+e^- \to \gamma\gamma$ is used for normalization. As a result of the normalization, a part of systematic uncertainties associated with event selection criteria for the process under study is canceled out. The accuracy of the luminosity measurement using $e^+e^- \to \gamma\gamma$ was studied in Ref. [12] and is estimated to be 1.4%.

TABLE I. The energy interval ($\sqrt{s}$), integrated luminosity (L), number of selected $e^+e^- \to K_S K_L \pi^0$ events (N), detection efficiency (ε), radiative correction factor ($1+\delta$), and the $e^+e^- \to K_S K_L \pi^0$ Born cross section (σ). The shown cross-section errors are statistical. The systematic error is 12%.

$\sqrt{s}$ (GeV)	L (nb^{-1})	N	ε	$1+\delta$	σ (nb)
1.300–1.350	2546	18 ± 7	0.058	0.872	0.14 ± 0.05
1.360–1.375	1468	10 ± 5	0.057	0.867	0.14 ± 0.06
1.400–1.440	2783	70 ± 10	0.057	0.851	0.52 ± 0.08
1.450–1.475	1082	48 ± 9	0.057	0.860	0.90 ± 0.16
1.500	2081	135 ± 13	0.055	0.867	1.35 ± 0.13
1.520–1.525	1437	105 ± 12	0.056	0.874	1.49 ± 0.18
1.550–1.575	1100	135 ± 13	0.056	0.886	2.48 ± 0.24
1.600–1.650	2997	408 ± 28	0.054	0.899	2.80 ± 0.19
1.675–1.700	2257	314 ± 22	0.053	0.923	2.85 ± 0.20
1.720–1.750	1575	180 ± 17	0.051	0.968	2.30 ± 0.21
1.760–1.800	3362	311 ± 26	0.049	1.039	1.81 ± 0.15
1.825–1.850	1973	109 ± 22	0.049	1.135	1.00 ± 0.23
1.870–1.900	3659	123 ± 15	0.049	1.249	0.55 ± 0.09
1.920–1.950	2667	23 ± 7	0.022	0.992	0.39 ± 0.12
1.960–2.000	2458	20 ± 7	0.020	0.974	0.41 ± 0.15

III. EVENT SELECTION

The reaction $e^+e^- \to K_S K_L \pi^0$ is studied in the $K_S \to \pi^0\pi^0$ decay mode. The K_L decay length is much larger than the radius of the SND calorimeter, and the length of its inelastic nuclear interaction is comparable with the calorimeter thickness [9]. In a significant fraction of $e^+e^- \to K_S K_L \pi^0$ events (25–30%), the K_L meson does not interact with the calorimeter, and only six photons from decays of three π^0 are detected. The K_L meson undergoing a nuclear interaction inside the detector produces one or several clusters in the calorimeter, which are reconstructed as photons.

The selection of $e^+e^- \to K_S K_L \pi^0$ events is based on finding three pairs of photons forming three π^0 candidates. Two of these π^0's having the invariant mass close to the K^0 mass form a K_S candidate. The events of the process under study are selected in two stages. The primary selection is based on the following criteria:

(i) No charged tracks are reconstructed in the drift chamber. The number of hits in the drift chamber is less than four.

(ii) The fired calorimeter crystals do not lie along a straight line. This requirement rejects cosmic-ray background.

(iii) An event contains at least six "good" photons ($N_\gamma \geq 6$) and no charged particles. A "good" photon is a cluster in the calorimeter with the energy deposition larger than 20 MeV, which has a transverse energy profile consistent with expectations for a photon [13]. The latter condition rejects spurious photons originating from K_L nuclear interaction or decay.

(iv) There are three π^0 candidates in an event. The π^0 candidate is a pair of photons with the invariant mass in the range from 110 to 160 MeV/c^2.

(v) The invariant mass of two π^0 candidates lies in the range 450–550 MeV/c^2.

The fraction of signal events rejected by the condition on the number of hits in the drift chamber varies between 6%

and 17%, depending on machine background conditions. It should be noted that the same condition is used for the selection of $e^+e^- \to \gamma\gamma$ events. Therefore, the possible systematic uncertainty due to this condition cancels as a result of the luminosity normalization.

For energies above 1.9 GeV, an additional selection criterion is applied to suppress the background from the process $e^+e^- \to K_S K_L \pi^0\pi^0$, $K_S \to \pi^0\pi^0$. Events containing more than three π^0 candidates selected with the mass window 100–170 MeV/c^2 are rejected.

The selected events are then kinematically fitted with three π^0 mass constraints and a K_S mass constraint. The χ^2 of the kinematic fit is required to be less than 15. The refined photon parameters are used to calculate the mass recoiling against the $K_S\pi^0$ system ($M_{\rm rec}$).

IV. ANALYSIS OF INTERMEDIATE STATES IN THE REACTION $e^+e^- \to K_S K_L \pi^0$

In Ref. [4] it was shown that the dominant mechanism of the $e^+e^- \to K_S K_L \pi^0$ reaction is the transition via the $K^*(892)^0\overline{K}^0$ intermediate state. The fraction of $e^+e^- \to \phi\pi^0 \to K_S K_L \pi^0$ events near the maximum of the $e^+e^- \to K_S K_L \pi^0$ cross section (1.7 GeV) is about 1% [3]. Also a small contribution of the $K_2^*(1430)^0\overline{K}^0$ state was observed in Ref. [4]. The $e^+e^- \to K_2^*(1430)\bar{K}$ cross section was measured in Ref. [3] in the charge modes $K^+K^-\pi^0$ and $K_S K^\pm\pi^\mp$. It proceeds in the D wave and is expected to be negligibly small in the VEPP-2000 energy region, below 2 GeV.

Figures 1 and 2 represent the distributions of the $K_{S(L)}\pi^0$ invariant mass (two entries per event) and the $K_S K_L$ invariant mass, respectively, for six-photon data events

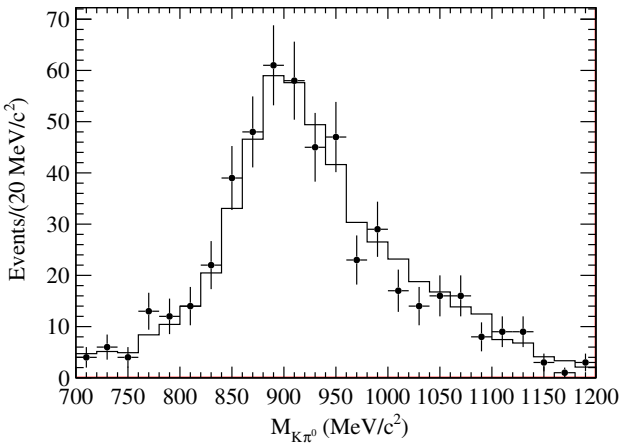

FIG. 1. The distribution of the invariant $K_L\pi^0$ and $K_S\pi^0$ masses (two entries per event) for data events from the energy region $\sqrt{s} = 1.600$–1.750 GeV (points with error bars). The histogram represents the simulated distributions obtained in the model with the $K^*(892)^0\bar{K}$ intermediate state.

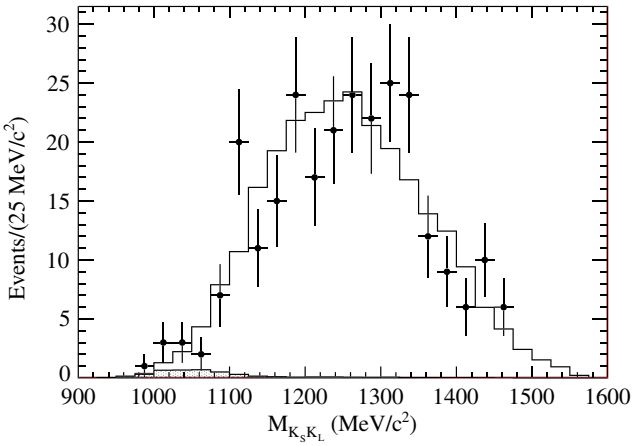

FIG. 2. The distribution of the $K_S K_L$ invariant mass for data events from the energy region $\sqrt{s} = 1.600$–1.750 GeV (points with error bars). The histogram represents the simulated distributions obtained in the model with the $K^*(892)^0\bar{K}$ intermediate state. The shaded histogram represents the expected contribution of the $e^+e^- \to \phi\pi^0$ process estimated using MC simulation.

from the energy region $\sqrt{s} = 1.600$–1.750 GeV selected with the extra condition $400 < M_{\rm rec} < 600$ MeV/c^2. Six-photon events are used to maximize the signal-to-background ratio. The fraction of background events in these distributions is estimated on the tails of the $M_{\rm rec}$ distribution (see Sec. V) and does not exceed 3%. It is seen that the data spectra in Figs. 1 and 2 are in good agreement with the simulated spectra obtained in the model with the $K^*(892)^0\overline{K}^0$ intermediate state. The shaded histogram in Fig. 2 represents the expected contribution of the $e^+e^- \to \phi\pi^0$ process estimated using MC simulation. With current statistics, we cannot observe the signal of the $\phi\pi^0$ intermediate state.

V. FIT TO THE $M_{\rm rec}$ SPECTRUM

The number of signal events is determined from the fit to the $M_{\rm rec}$ spectrum (Fig. 3) by a sum of distributions for signal and background events. The signal distribution is described by a sum of three Gaussian functions with parameters determined from the fit to the simulated signal $M_{\rm rec}$ spectrum. To account for a possible inaccuracy of the signal simulation, two parameters are introduced: mass shift ΔM and smearing parameter $\Delta\sigma^2$. The latter is added to all Gaussian sigmas squared ($\sigma_i^2 \to \sigma_i^2 + \Delta\sigma^2$). The parameters ΔM and $\Delta\sigma^2$ are determined from the fit to the $M_{\rm rec}$ spectrum for events from the energy range $\sqrt{s} =$ 1.6–1.75 GeV shown in Fig. 3. They are found to be $\Delta M = (5 \pm 5)$ MeV/c^2 and $\Delta\sigma^2 = 1800 \pm 770$ MeV^2/c^4.

To obtain the background distribution we analyze simulation for the processes $e^+e^- \to K_S K_L$, $e^+e^- \to K_S K_L \pi^0\pi^0$, $e^+e^- \to \phi\eta$, $e^+e^- \to \omega\pi^0$, $e^+e^- \to \omega\eta$, $e^+e^- \to \omega\pi^0\pi^0$,

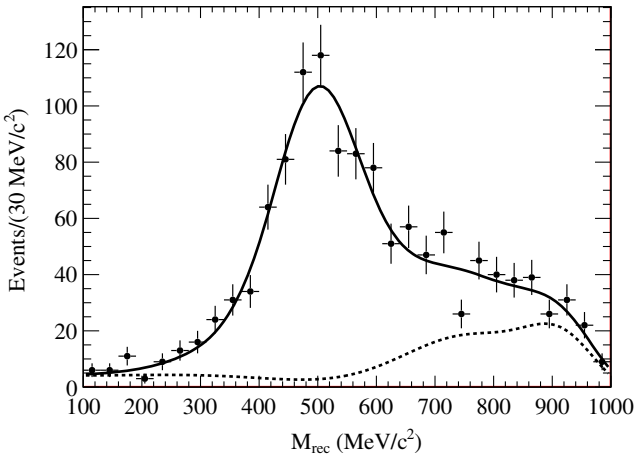

FIG. 3. The spectrum of the mass recoiling against the $K_S\pi^0$ system for data events from the energy region $\sqrt{s} = 1.60$–1.75 GeV. The solid curve represents the result of the fit to the spectrum with a sum of signal and background distributions. The dashed curve represents background distribution.

and $e^+e^- \to \omega\pi^0\eta$, with decays $\phi \to K_SK_L$ and $\omega \to \pi^0\gamma$. For all of these processes, the existing experimental data on Born cross sections are approximated and then used in event generators for the calculation of radiative corrections and the generation of extra photons emitted from the initial state. The obtained simulated background distribution is fitted with a smooth function. The largest contributions into expected background come from the processes $e^+e^- \to K_SK_L$ and $e^+e^- \to K_SK_L\pi^0\pi^0$.

In the fit to the data $M_{\rm rec}$ spectra, the background distribution obtained from simulation is multiplied by a free scale factor. For all energy regions, the fitted value of the scale factor was found to be consistent with unity. The example of the fit for the energy region $\sqrt{s} =$ 1.60–1.75 GeV is presented in Fig. 3.

Some fraction of selected signal events contains a hard photon emitted from the initial state. These initial-state-radiation (ISR) events have $M_{\rm rec}$ larger than the K^0 mass and distort the shape of the signal $M_{\rm rec}$ distribution. The distortion is most significant at energies $\sqrt{s} > 1.92$ GeV, where the fraction of ISR events becomes larger than 50%. For these energies, the fitting procedure is modified. The signal spectrum is represented as a sum of two spectra, for events with the photon energy E_γ smaller and larger than 120 MeV. The number of events in the latter spectrum and its error are calculated using the Born $e^+e^- \to K_SK_L\pi^0$ cross section measured in this work in the lower-energy interval. The number of signal events with $E_\gamma < 120$ MeV is determined from the fit to the data $M_{\rm rec}$ spectrum.

The fitted numbers of signal events obtained for 15 energy intervals are listed in Table I.

VI. DETECTION EFFICIENCY

The detection efficiency for $e^+e^- \to K_SK_L\pi^0$ events is determined using MC simulation. The simulation takes into account radiative corrections [14], in particular, the emission of an extra photon from the initial state [15]. The Born cross section for the process $e^+e^- \to K_SK_L\pi^0$ is taken from Ref. [4].

The detection efficiency obtained from MC simulation is corrected to take into account the difference between data and simulation in photon conversion in detector material before the tracking system. This difference is measured using $e^+e^- \to \gamma\gamma$ events. The conversion probability for two photons is canceled when normalizing to luminosity. The remaining data-MC simulation difference for four photons is $-(1.35 \pm 0.05)\%$ [16].

We also study the data-simulation difference in the photon transverse energy-deposition profile in the calorimeter. To do this, $e^+e^- \to \omega\pi^0 \to \pi^0\pi^0\gamma \to 5\gamma$ events are used, which can be selected without background [12]. The dependence of the photon loss due to the "good" photon requirement on the photon energy is measured in data and simulation. The obtained data-simulation difference is used to determine the efficiency correction for simulated $e^+e^- \to K_SK_L\pi^0$ events. The correction is found to be practically independent of $\sqrt{s}$ and is equal to $-(3.4 \pm 1.3)\%$.

A high-statistics study of the systematic uncertainty associated with the selection of multiphoton events based on the kinematic fit was performed in Refs. [12,17] using $e^+e^- \to \omega\pi^0 \to \pi^0\pi^0\gamma$ events. We estimate that the systematic uncertainty due to conditions on invariant masses and χ^2 of the kinematic fit does not exceed 5%.

The detection efficiency calculated in the model of the $K^*(892)^0\overline{K}^0$ intermediate state ($\varepsilon_{K^*\bar{K}}$) is modified to take into account a small contribution of the $\phi\pi^0$ intermediate state:

$$\varepsilon = \varepsilon_{K^*\bar{K}}\left(1 + \frac{\varepsilon_{\phi\pi^0} - \varepsilon_{K^*\bar{K}}}{\varepsilon_{K^*\bar{K}}} f_{\phi\pi^0}\right), \qquad (1)$$

where $\varepsilon_{\phi\pi^0}$ is the detection efficiency for the process $e^+e^- \to \phi\pi^0 \to K_SK_L\pi^0$, and $f_{\phi\pi^0}$ is the ratio of the $e^+e^- \to \phi\pi^0 \to K_SK_L\pi^0$ cross section [3] and the total $e^+e^- \to K_SK_L\pi^0$ cross section obtained in this work. The relative difference $(\varepsilon_{\phi\pi^0} - \varepsilon_{K^*\bar{K}})/\varepsilon_{K^*\bar{K}}$ varies in the range 10–30%. The efficiency correction is 0.1–0.7% in the range 1.40–1.85 GeV and about 2% above and about 3% below this interval. The associated systematic uncertainty is determined by the accuracy of the $e^+e^- \to \phi\pi^0$ cross section [3] and does not exceed 0.6% in the range 1.4–1.9 GeV, and it is 2% above and below. The maximum possible contribution of the $K_2^*(1430)^0\overline{K}^0$ mechanism can be estimated from the measurement of the isovector and

isoscalar $e^+e^- \to K_2^*(1430)^0\overline{K}^0$ cross sections in Ref. [3] and isospin relations [18] assuming constructive interference of the isovector and isoscalar amplitudes. It does not exceed 10% of the total $e^+e^- \to K_S K_L \pi^0$ cross section at $\sqrt{s} > 1.9$ GeV and it is negligible below. The detection efficiency for $e^+e^- \to K_2^*(1430)^0\overline{K}^0 \to K_S K_L \pi^0$ events is about 40% larger than $\varepsilon_{K^*\bar{K}}$. Therefore, we estimate that the systematic uncertainty on the detection efficiency due to the possible contribution of the $K_2^*(1430)^0\overline{K}^0$ mechanism does not exceed 4% at $\sqrt{s} > 1.9$ GeV.

The corrected detection efficiencies for the 15 energy regions are listed in Table I. For the two intervals with $\sqrt{s} > 1.92$ GeV, the efficiency is calculated with the additional requirement $E_\gamma < 120$ MeV. The systematic uncertainty on detection efficiency is 5.2% in the range $\sqrt{s} = 1.4$–1.9 GeV, 5.5% at $\sqrt{s} < 1.4$ GeV, and 6.8% at $\sqrt{s} > 1.9$ GeV.

VII. THE BORN CROSS SECTION

The visible cross section for the process $e^+e^- \to K_S K_L \pi^0$ is obtained from data as

$$\sigma_{\mathrm{vis},i} = \frac{N_i}{\varepsilon_i L_i}, \tag{2}$$

where N_i is the number of $K_S K_L \pi^0$ events obtained from the fit to the M_{rec} spectrum in Sec. V, ε_i is the detection efficiency, and L_i is the integral luminosity for the ith energy region.

The Born cross section σ relates to the visible cross section as

$$\sigma_{\mathrm{vis}}(\sqrt{s}) = \int_0^{x_{\max}} W(s,x)\sigma\Big(\sqrt{s(1-x)}\Big)dx, \tag{3}$$

where $W(s,x)$ is the so-called radiator function, which describes the probability of emission of photons with the energy $x\sqrt{s}/2$ by the initial electron and positron [14].

Equation (3) can be represented as

$$\sigma_{\mathrm{vis}}(\sqrt{s}) = \sigma(\sqrt{s})[1+\delta(\sqrt{s})], \tag{4}$$

where $\delta(\sqrt{s})$ is the radiation correction, which is calculated as a result of the fit to the visible-cross-section data with Eq. (3) and a theoretical model for the Born cross section. The vector-meson dominance (VMD) model [19] is used to describe the energy dependence of the $e^+e^- \to K_S K_L \pi^0$ cross section. In principle, it should include contributions of all vector resonances of the ρ, ω, and ϕ families. In Ref. [3] it is shown that the isoscalar contribution dominates only near the maximum of the $\phi(1680)$ resonance. Below 1.55 GeV and above 1.8 GeV, the isoscalar and isovector amplitudes are the same order of magnitude. However, for the purpose of calculating the radiation correction, a simple model with the $\phi(1020)$ and $\phi(1680)$ resonances is sufficient. This model describes the experimental data well. However, its fitted parameters should not be considered when measuring the parameters of the $\phi(1020)$ and $\phi(1680)$ resonances. The Born cross section for the process $e^+e^- \to K_S K_L \pi^0$ is described by the following formula:

$$\sigma(\sqrt{s}) = |A_0(s) + e^{i\alpha}A_1(s)|^2 \frac{P(s)}{s^{3/2}}, \tag{5}$$

where A_0 and A_1 are the amplitudes of the $\phi(1020)$ and $\phi(1680)$ decays to $K_S K_L \pi^0$, and α is their relative phase. It was assumed that the decays proceed via the $K^*(892)^0\overline{K}^0$ intermediate state. So, the function $P(s)$ describes the energy dependence of the $K^*(892)^0\overline{K}^0$ phase space [19],

$$P(s) = \frac{1}{\pi}\int_{(m_{\pi^0}+m_{K^0})^2}^{(\sqrt{s}-m_{K^0})^2} \frac{m_{K^*}\Gamma_{K^*}}{(q^2-m_{K^*}^2)^2 + m_{K^*}^2\Gamma_{K^*}^2} p^3(q^2)dq^2,$$
$$p(q^2) = \sqrt{\frac{(s-m_{K^*}^2-q^2)^2 - 4m_{K^*}^2 q^2}{4s}}, \tag{6}$$

where m_{K^*} and Γ_{K^*} are the $K^*(892)^0$ mass and width [20], and $p(q^2)$ is the momentum of the $K^0\pi^0$ system.

The $\phi(1020)$ amplitude is parametrized as

$$A_0(s) = A_\phi \frac{M_\phi \Gamma_\phi}{(M_\phi^2 - s) - i\sqrt{s}\Gamma_\phi}, \tag{7}$$

where A_ϕ is a real constant and M_ϕ and Γ_ϕ are the $\phi(1020)$ mass and width, respectively [20], while the $\phi' \equiv \phi(1680)$ amplitude is given by

$$A_1(s) = \sqrt{\frac{\sigma_{\phi'} M_{\phi'}^3}{P(M_{\phi'})}} \frac{M_{\phi'}\Gamma_{\phi'}}{(M_{\phi'}^2 - s) - i\sqrt{s}\Gamma_{\phi'}}, \tag{8}$$

where $\sigma_{\phi'}$ is the cross section of the process $e^+e^- \to \phi' \to K_S K_L \pi^0$ at $\sqrt{s} = M_{\phi'}$, and $M_{\phi'}$ and $\Gamma_{\phi'}$ are the ϕ' mass and width, respectively. The free fit parameters are A_ϕ, $\sigma_{\phi'}$, α, $M_{\phi'}$, and $\Gamma_{\phi'}$. The model describes data well ($\chi^2/\mathrm{ndf} = 7/15$, where ndf is the number of degrees of freedom). The fitted ϕ' mass (1700 ± 23 MeV/c^2) and width (300 ± 50 MeV) are close to the Particle Data Group values for $\phi(1680)$ [20].

The radiation corrections calculated with the fitted model parameters are listed in Table I. The experimental values of the Born cross section are then obtained from the measured values of the visible cross sections using Eq. (4). They are listed in Table I and shown in Fig. 4 together with the fitted curve.

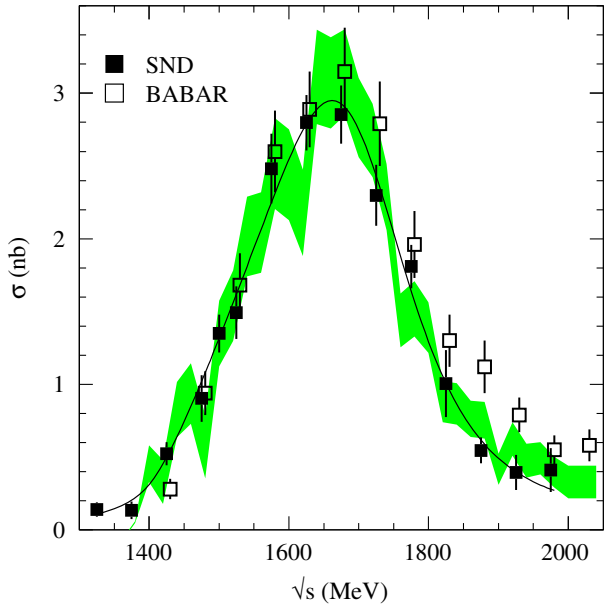

FIG. 4. The Born cross section for the process $e^+e^- \to K_S K_L \pi^0$ measured in this work (filled squares) in comparison with the *BABAR* data [4] (open squares). The curve represents the result of the fit to SND data with the VMD model. The band represents the prediction for the $e^+e^- \to K_S K_L \pi^0$ cross section obtained using isospin relations from the *BABAR* measurements of the $e^+e^- \to K_S K^\pm \pi^\mp$, $e^+e^- \to K^+K^-\pi^0$, and $e^+e^- \to \phi\pi^0$ cross sections [3].

VIII. SYSTEMATIC UNCERTAINTY

Several sources give contributions to the systematic uncertainty of the measured cross section. These are the uncertainties of luminosity measurement and detection efficiency, the systematic uncertainty in determination of the number of signal events from the fit to the $M_{\rm rec}$ spectrum, and the model uncertainty of the radiative correction.

A possible source of the systematic uncertainty on the number of signal events is imperfect simulation of the shape of the signal and background $M_{\rm rec}$ distributions.

In the fit to the $M_{\rm rec}$ spectrum, we use the simulated background distribution multiplied by a free scale factor. To estimate the systematic uncertainty due to imperfect simulation of the background shape, another approach to background description is applied, by a sum of predicted background plus a linear function. The difference in the number of signal events obtained with the standard and new background descriptions does not exceed 5% in the energy region 1.60–1.75 GeV. This value is used as an estimate of the uncertainty.

The signal $M_{\rm rec}$ distribution has an asymmetric line shape (see Fig. 3). The tail of the distribution at $M_{\rm rec} > m_{K^0}$ originates from events with $N_\gamma > 6$, in which the wrong combination of photons forming the $K_S\pi^0$ system is chosen. For six-photon events, the line shape is symmetric and close to Gaussian. To estimate the systematic uncertainty associated with the signal line shape, we repeat the analysis, selecting events with $N_\gamma = 6$. The visible cross section near the maximum is found to be $(20 \pm 5)\%$ lower than the cross section obtained with the standard selection criteria. The observed difference is partly explained by incorrect simulation of K_L nuclear interaction. At the K_L energy 510 MeV, the inelastic nuclear interaction length used in simulation [10] is larger than the measured one by $(12 \pm 5)\%$. The six-photon selection in contrast to the standard selection is very sensitive to the value of the K_L nuclear interaction length: its decrease by 12% is translated to the 11% decrease of the detection efficiency [21]. The remaining difference $(9 \pm 7)\%$ is used as an estimate of the uncertainty associated with the signal line shape.

TABLE II. The systematic uncertainties (%) on the measured $e^+e^- \to K_S K_L \pi^0$ Born cross section in four c.m. energy intervals.

Source	1.3–1.4 GeV	1.40–1.8 GeV	1.8–1.9 GeV	1.9–2.0 GeV
Luminosity	1.4	1.4	1.4	1.4
Detection efficiency	5.5	5.2	5.2	6.8
Background subtraction	5.0	5.0	5.0	5.0
Signal line shape	9.0	9.0	9.0	9.0
Radiative corrections	0.5	0.5–1.2	1.9–2.4	2.6–3.5
Total	12	12	12	13

The model uncertainty of the radiation correction is estimated by varying the fitted parameters of the VMD model [Eqs. (5)–(8)] within their errors. It is below 0.5% at $\sqrt{s} < 1.65$ GeV and increases up to 3.5% near 2 GeV. The systematic uncertainty on the detection efficiency is discussed in Sec. VI and is 5.2% in the range $\sqrt{s} =$ 1.4–1.9 GeV, 5.5% at $\sqrt{s} < 1.4$ GeV, and 6.8% at $\sqrt{s} > 1.9$ GeV. The systematic uncertainty of the luminosity measurement studied in Refs. [12,17] is 1.4%.

The systematic uncertainties from different sources are summarized in Table II for four c.m. energy intervals. The total systematic uncertainty including all the contributions discussed above combined in quadrature is estimated to be 12% below 1.9 GeV and 13% above.

IX. DISCUSSION AND SUMMARY

The cross section for the process $e^+e^- \to K_S K_L \pi^0$ has been measured with the SND detector at the VEPP-2000 e^+e^- collider in the energy range 1.3–2.0 GeV. The comparison of the SND data with the only previous measurement, done by the *BABAR* Collaboration [4], is presented in Fig. 4. Only statistical errors are shown. The systematic uncertainty of the SND data is 12–13%, while the *BABAR* systematic uncertainty increases from 10% at 1.7 GeV and below to about 20% at 2 GeV [4]. Near the maximum of the cross section (1.7 GeV), the SND points

lie below the *BABAR* points, but agree within systematic errors. The same trend persists at higher energies, up to 2 GeV. The largest difference, about 2 standard deviations including systematic uncertainties, between the SND and *BABAR* data is observed in the energy points 1.875 and 1.925 GeV.

It is discussed in Sec. IV that the dominant mechanism of the $e^+e^- \to K_S K_L \pi^0$ reaction at $\sqrt{s} < 2$ GeV is $K^*(892)^0 \bar{K}$. Under this assumption, the cross section of the process under study can be predicted using the isospin relation [18]

$$\begin{aligned}\sigma(e^+e^- \to K_S K_L \pi^0) &= \sigma(e^+e^- \to K_S K^\pm \pi^\mp) - \sigma(e^+e^- \to K^+K^-\pi^0) \\ &+ B(\phi \to K\bar{K})\sigma(e^+e^- \to \phi\pi^0) \end{aligned} \quad (9)$$

and the *BABAR* measurements [3] of the $e^+e^- \to K_S K^\pm \pi^\mp$, $e^+e^- \to K^+K^-\pi^0$, and $e^+e^- \to \phi\pi^0$ cross sections. In Eq. (9) we take into account that both $\sigma(e^+e^- \to K_S K_L \pi^0)$ and $\sigma(e^+e^- \to K^+K^-\pi^0)$ contain contributions of the $\phi\pi^0$ intermediate state. The predicted cross section is shown in Fig. 4 by the green band and is found to be in good agreement with our measurement.

ACKNOWLEDGMENTS

This work is supported by the Russian Foundation for Basic Research Grants No. 16-02-00014 and No. 16-02-00327. Part of this work related to the photon reconstruction algorithm in the electromagnetic calorimeter for multiphoton events is supported by the Russian Science Foundation (Project No. 14-50-00080).

[1] F. Mane *et al.*, Phys. Lett. **112B**, 178 (1982).
[2] D. Bisello, Nucl. Phys. B, Proc. Suppl. **21**, 111 (1991).
[3] B. Aubert *et al.* (*BABAR* Collaboration), Phys. Rev. D **77**, 092002 (2008).
[4] J. P. Lees *et al.* (*BABAR* Collaboration), Phys. Rev. D **95**, 052001 (2017).
[5] M. N. Achasov *et al.*, Nucl. Instrum. Methods Phys. Res., Sect. A **598**, 31 (2009); V. M. Aulchenko *et al.*, Nucl. Instrum. Methods Phys. Res., Sect. A **598**, 102 (2009); A. Yu. Barnyakov *et al.*, Nucl. Instrum. Methods Phys. Res., Sect. A **598**, 163 (2009); V. M. Aulchenko *et al.*, Nucl. Instrum. Methods Phys. Res., Sect. A **598**, 340 (2009).
[6] A. Romanov *et al.*, in *Proceedings of PAC 2013, Pasadena, CA USA*, p. 14.
[7] E. A. Kuraev and Z. K. Silagadze, Phys. At. Nucl. **58**, 1589 (1995).
[8] GEANT4 Physics Reference Manual, in http://cern.ch/geant4/support/userdocuments.shtml.
[9] M. N. Achasov *et al.* (SND Collaboration), J. Instrum. **10**, P09006 (2015).
[10] R. Baldini and A. Michetti, Report No. LNF-96/008, 1996.
[11] G. A. Sayer, E. F. Beall, T. J. Devlin, P. Shepard, and J. Solomon, Phys. Rev. **169**, 1045 (1968).
[12] M. N. Achasov *et al.* (SND Collaboration), Phys. Rev. D **94**, 112001 (2016).
[13] A. V. Bozhenok, V. N. Ivanchenko, and Z. K. Silagadze, Nucl. Instrum. Methods Phys. Res., Sect. A **379**, 507 (1996).
[14] E. A. Kuraev and V. S. Fadin, Yad. Fiz. **41**, 733 (1985) [Sov. J. Nucl. Phys. **41**, 466 (1985)].
[15] G. Bonneau and F. Martin, Nucl. Phys. **B27**, 381 (1971).
[16] M. N. Achasov *et al.* (SND Collaboration), Phys. Rev. D **94**, 092002 (2016).
[17] M. N. Achasov *et al.* (SND Collaboration), Phys. Rev. D **88**, 054013 (2013).
[18] M. Davier, A. Hoecker, B. Malaescu, and Z. Zhang, Eur. Phys. J. C **71**, 1515 (2011); **72**, 1874(E) (2012).
[19] N. N. Achasov and A. A. Kozhevnikov, Phys. Rev. D **57**, 4334 (1998).
[20] C. Patrignani *et al.* (Particle Data Group), Chin. Phys. C **40**, 100001 (2016).
[21] L. A. Korneev, Master's thesis, Novosibirsk State University, 2017.